0026-895X/01/6005-1008–1019$3.00
MOLECULAR PHARMACOLOGY
Copyright © 2001 The American Society for Pharmacology and Experimental Therapeutics
Mol Pharmacol 60:1008–1019, 2001

Vol. 60, No. 5
727/936158
Printed in U.S.A.

Multiple Kinetics of Mitochondrial Cytochrome *c* Release in Drug-Induced Apoptosis

C. MARC LUETJENS, DONAT KÖGEL, CLAUS REIMERTZ, HEIKO DÜßMANN, ANDREA RENZ, KLAUS SCHULZE-OSTHOFF, ANNA-LIISA NIEMINEN, MONIKA POPPE, and JOCHEN H. M. PREHN

Interdisciplinary Center for Clinical Research, Research Group "Apoptosis and Cell Death" (C.M.L., D.K., C.R., H.D., M.P., J.H.M.P.), Division of Immunology and Cell Biology, Department of Experimental Dermatology (A.R., K.S.-O.), and Department of Pharmacology and Toxicology (J.H.M.P.), Westphalian Wilhelms-University, Münster, Germany; and Department of Anatomy, School of Medicine, Case Western Reserve University, Cleveland, Ohio (A.-L.N.)

Received November 30, 2000; accepted July 16, 2001

This paper is available online at http://molpharm.aspetjournals.org

ABSTRACT

We investigated cytochrome *c* release kinetics in response to three apoptosis-inducing agents (tumor necrosis factor-α, staurosporine, and valinomycin) in MCF-7/Casp-3 cells stably transfected with enhanced green fluorescent protein (EGFP)-tagged cytochrome *c*. All three agents induced significant caspase activation in the cultures determined by monitoring the cleavage of fluorigenic caspase substrates in extracts from drug-treated MCF-7/Casp-3 cells, albeit the valinomycin-induced activation was less pronounced. Time-lapse confocal microscopy showed that tumor necrosis factor-α and staurosporine caused rapid, one- or multiple-step release of cytochrome *c*-EGFP from mitochondria. In contrast, valinomycin-induced cytochrome *c*-EGFP release occurred slowly over several hours. Unlike staurosporine, the valinomycin-induced cytochrome *c* release was not associated with translocation of the proapoptotic Bax protein to the mitochondria, and was not accompanied by co-release of the proapoptotic Smac protein. Immunoprecipitation experiments revealed that cytochrome *c* was also released out of the cell into the extracellular space before loss of plasma membrane integrity. Our data indicate the existence of multiple kinetics of cytochrome *c* release in drug-induced apoptosis.

Numerous cytokines and cytotoxic drugs are able to activate an evolutionary conserved cell death program, resulting in apoptosis. The release of cytochrome *c* from the mitochondrial intermembrane space into the cytosol represents a central coordinating step in this program (Liu et al., 1996). Cytoplasmic cytochrome *c* is able to induce a caspase-3 activating complex, composed of cytochrome *c*, Apaf-1, dATP, and procaspase-9 (Li et al., 1997b; Zou et al., 1997). Activation of caspases is responsible for most of the biochemical and morphological changes accompanying apoptosis.

In the so-called extrinsic pathway, the upstream caspase-8 is activated after ligand binding to death receptors (Krammer, 1999). Caspase-8 subsequently activates downstream caspases, but also cleaves Bid, a proapoptotic, Bcl-2-homology-3-domain-only Bcl-2 family member (Li et al., 1998; Luo et al., 1998). The truncated form tBid induces cytochrome *c* release from mitochondria and thereby amplifies the apoptotic signal (Li et al., 1998; Luo et al., 1998). In the intrinsic pathway, release of cytochrome *c* from mitochondria occurs independent of upstream caspases (Bossy-Wetzel et al., 1998). Here, cytochrome *c* release is required for caspase activation (Li et al., 2000). The proapoptotic Bcl-2 family proteins Bax and Bak have been shown to be involved in cytochrome *c* release in both apoptotic pathways (Goping et al., 1998; Desagher et al., 1999; Perez and White, 2000; Wei et al., 2000, 2001).

Opening of the outer mitochondrial membrane is necessary for the release of cytochrome *c*. The precise release mechanisms in apoptosis are still controversial. Several theories argue for selective opening of pores of the outer mitochondrial membrane (Eskes et al., 1998; Kluck et al., 1999). Two models concerning the structural composition of these outer membrane pores have been suggested: according to the first model, the channel is formed by oligomerization of Bax or Bak proteins (Saito et al., 2000), whereas the second model argues for a channel consisting of Bax and the voltage-dependent anion channel (VDAC) (Shimizu et al., 1999). A different theory implies opening of the inner and outer mitochondrial membranes after the induction of a mitochondrial

Supported by IZKF Universität Münster Grant BMBF 01 KS 9604/0 (to J.H.M.P.).

C.M.L. and D.K. contributed equally to this work.

ABBREVIATIONS: VDAC, voltage-dependent anion channel; PTP, permeability transition pore; EGFP, enhanced green fluorescent protein; TNF-α, tumor necrosis factor-α; CHX, cycloheximide; Ac-DEVD-AMC, acetyl-Asp-Glu-Val-Asp-aminomethylcoumarin; STS, staurosporine; DTT, dithiothreitol; CHAPS, 3-(3-cholamidopropyldimethylammonio)-1-propane sulfonate; DMSO, dimethyl sulfoxide; IAP, inhibitor of apoptosis protein.

megachannel, the so-called permeability transition pore (PTP) (Marzo et al., 1998; Lemasters et al., 1999).

In the present study, we analyzed cytochrome *c* release kinetics in cells stably expressing cytochrome *c* tagged with enhanced green fluorescent protein (EGFP) utilizing three distinct apoptotic stimuli: 1) tumor necrosis factor-α (TNF-α) plus cycloheximide (CHX), a stimulant of death receptor-mediated apoptosis (Krammer, 1999); 2) exposure to the protein kinase inhibitor staurosporine, which has been shown to release cytochrome *c* via the intrinsic pathway (Li et al., 2000); and 3) exposure to valinomycin, a K^+ ionophore that has been shown to depolarize mitochondria and to trigger PTP opening (Inai et al., 1997; Furlong et al., 1998). The data presented here demonstrate that cytochrome *c* release in apoptosis reveals multiple kinetics depending on the type of stimulus.

Experimental Procedures

Materials. Recombinant human TNF-α, CHX, valinomycin, and embryo-tested paraffin oil were purchased from Sigma Chemie (Deisenhofen, Germany). Staurosporine (STS) was from Alexis Corporation (Läufelfingen, Switzerland) and caspase substrate, acetyl-Asp-Glu-Val-Asp-aminomethylcoumarin (Ac-DEVD-AMC), was purchased from Bachem (Bubendorf, Switzerland). All other chemicals came in analytical grade purity from Merck (Darmstadt, Germany).

Cell Culture and Transfection. Human breast carcinoma MCF-7/Casp-3 cells stably transfected with caspase-3 (Jänicke at al., 1998) were cultured in RPMI 1640 medium (Invitrogen, Carlsbad, CA) supplemented with penicillin (100 U/ml), streptomycin (100 μg/ml), and 10% fetal calf serum (PAA Laboratories GmbH, Cölbe, Germany). For transfection, MCF-7/Casp-3 cells were plated onto 12.5-cm^2 culture flasks. Cells cultured for 24 h were transfected with a plasmid for cytochrome *c*-EGFP (Heiskanen et al., 1999) using the F2 transfection reagent (Targeting Systems, Santee, CA). Five micrograms of DNA and 5 μl of F2-reagent were diluted in 2.5 ml of RPMI medium under serum-free conditions and incubated at 37°C for 20 min. The cultures were then incubated with the DNA-F2-transfection mixture at 37°C for 2 h. Cells were cultured overnight with RPMI medium containing 10% fetal calf serum. For the generation of stable cell lines, transfected MCF-7/Casp-3 cells were selected in the presence of 1 mg/ml G418 for 2 weeks, and clones expressing mitochondrial cytochrome *c*-EGFP were enriched. Expression of cytochrome *c*-EGFP was verified by immunoblotting using antibodies against GFP and cytochrome *c* as described below (see also Heiskanen et al., 1999). Epifluorescence and confocal microscopy revealed that the cytochrome *c*-EGFP fluorescence signal colocalized with a Mitotracker Red or tetramethylrhodamine ethyl ester uptake signal (Heiskanen et al., 1999 and data not shown). The growth properties and mitochondrial membrane potential of MCF-7/Casp-3 cytochrome *c*-EGFP cells were similar to the parental control cell line. To generate pDsRed1-N1-bax, the complete open reading frame (codon 1–192) of human Bax-α was amplified with primers 5′-TTAGATCTATGGACGGGTCCGGGGAG-3′ and 5′-AAGAATTCCCATCTTCTTCCAGATGGTGA-3′ using Pfu Polymerase (Promega, Charbonnières, France). The PCR-obtained product was then digested with *Bgl*II and *Eco*RI and cloned between the *Bgl*II and *Eco*RI sites of pDsRed1-N1 (CLONTECH, Palo Alto, CA). The MCF-7/DsRed-bax cell line was established by cotransfection of pDsRed1-N1-bax with a puromycin resistance plasmid and selection with 1 μg/ml puromycin for 6 weeks.

Epifluorescence Microscopy. Cytochrome *c*-EGFP-expressing cells were cultivated at least overnight in 150 μl of medium on 35-mm glass-bottom dishes (Willco BV, Amsterdam, The Netherlands) coated with poly-L-lysine to let them attach firmly. EGFP fluorescence was observed using an Eclipse TE 300 inverted microscope and a 100× oil immersion objective (Nikon, Düsseldorf, Germany) equipped with the appropriate filter set (excitation, 490 nm; dichroic mirror, 505 nm; and emission, >510 nm). DsRed-bax-expressing cells were analyzed with the Eclipse TE 300 inverted microscope and a 40× oil immersion objective. DsRed fluorescence was observed with the following optics: excitation, 510 to 560 nm; dichroic mirror, 575 nm; and emission, >590 nm. Digital images of equal exposure were acquired with a SPOT-2 camera using Spot software version 2.2.1 (Diagnostic Instruments, Sterling Heights, MI).

Time-Lapse Confocal Fluorescence Microscopy. Cytochrome *c*-EGFP was monitored and quantified confocally using an inverted Olympus IX70 microscope attached to a confocal laser scanning unit equipped with a 488-nm argon laser and a 60× oil fluorescence objective (Fluoview; Olympus, Hamburg, Germany). For time-lapse images, dishes were mounted onto a microscope stage equipped with a temperature-controlled inlay HT200 (Minitüb, Tiefenbach, Germany). In control experiments, the cytochrome *c*-EGFP signal was monitored for up to 24 h. Cells were incubated with 100 ng/ml TNF-α plus 1 μg/ml cycloheximide (TNF-α/CHX), 3 μM STS, or 10 μM valinomycin directly on the stage after acquiring the first image. Controls were exposed to vehicle (phosphate-buffered saline in the case of TNF-α/CHX, dimethyl sulfoxide in the case of STS and valinomycin). The medium was enriched with 10 mM Hepes (pH 7.4) and thoroughly mixed to ensure a proper distribution of the drugs. To prevent evaporation the media was covered with embryo-tested paraffin oil. Data were obtained using Fluoview 2.0 software (Olympus), Kalman-filtered from four individual scans for each time point, and averaged. Quantitative analysis of the data was performed using Metamorph software (Universal Imaging Cooperation, Downingtown, PA). For each individual cell, mitochondria-rich and nuclear regions were defined separately employing merged fluorescence and brightfield images. Fluorescence data are given as the average pixel intensity of the mitochondria-rich regions or of the nucleus.

Digitonin Permeabilization. Selective permeabilization of MCF-7/Casp-3 cytochrome *c*-EGFP cells with digitonin was used to analyze the co-release of cytochrome *c* and cytochrome *c*-EGFP from mitochondria. This method obviates possible artifacts due to mechanical breakage of the outer mitochondrial membrane by dounce homogenization. Culture plates with 10^6 cells per well were placed on ice, and the culture medium was removed. The cells were washed once with ice-cold phosphate-buffered saline (PBS) and subsequently incubated in 100 μl of permeabilization buffer (210 mM D-mannitol, 70 mM sucrose, 10 mM Hepes, 5 mM succinate, 0.2 mM EGTA, and 250 μg/ml digitonin, pH 7.2). At the indicated time points the permeabilization buffer was transferred to a reaction tube and centrifuged for 10 min at 13,000*g*. Subsequently, the supernatant was transferred to a new reaction tube and denatured in SDS-loading buffer. Equal amounts of protein were analyzed by Western blot analysis using 15% polyacrylamide gels as described below. Control experiments were carried out by incubation of cells with permeabilization buffer devoid of digitonin and revealed no release of cytochrome *c* or cytochrome *c*-EGFP.

Preparation of Cytosolic and Mitochondria-Enriched Fractions and Western Blotting. Cells from one 175-cm^2 flask were collected at 200*g* for 5 min and washed with PBS. The cell pellet was resuspended in 100 μl of buffer A [20 mM Hepes-KOH, pH 7.5, 10 mM KCl, 1.5 mM $MgCl_2$, 1 mM EGTA, 1 mM dithiothreitol (DTT), 250 mM sucrose, 100 mM phenylmethylsulfonyl fluoride, 1 μg/ml pepstatin A, 2 μg/ml leupeptin, and 2 μg/ml aprotinin]. Cells were homogenized using a glass dounce homogenizer and a tight pestle (10 strokes). Cell homogenates were centrifuged at 15,000*g* for 15 min at 4°C. The supernatant was respun for a further 15 min at 20,000*g* at 4°C. The pellet obtained from the first centrifugation step represented the mitochondria-enriched fraction; the second supernatant represented the cytoplasmic extract. Protein content was determined with the Pierce Micro-BCA Protein Assay Kit (KMF, Cologne, Germany). Thirty micrograms of protein was loaded onto a 15% SDS-

polyacrylamide gel. Proteins were separated for 1 h at 120 V and then blotted to nitrocellulose membranes (Protean BA 83; 2 μm; Schleicher & Schuell, Dassel, Germany) in Towbin buffer [25 mM Tris, 192 mM glycine, 20% methanol (v/v), and 0.01% SDS] at 15 V for 45 min. The blots were blocked with 5% nonfat milk in TBST (15 mM Tris-HCl, pH 7.5, 200 mM NaCl, and 0.1% Tween-20) for 2 h at room temperature. Membranes were incubated with a mouse monoclonal anti-cytochrome *c* antibody (clone 7H8.2C12, 1:1000; BD Pharmingen, Hamburg, Germany), a mouse monoclonal anti-GFP antibody (1:1000; CLONTECH), a rabbit polyclonal anti-Bid antiserum (1:1000; Trevigen, Gaithersburg, MD), a rabbit polyclonal anti-Bax antiserum (1:1000; Upstate Biotechnology, Lake Placid, NY), a rat monoclonal anti-Smac/Diablo antibody (clone 10G7, 1:1000, Alexis Corporation), a mouse monoclonal anti-VDAC antibody (clone 31HL, 1:1000; Calbiochem, Bad Soden, Germany) to exclude contamination of cytoplasmic extracts with mitochondrial

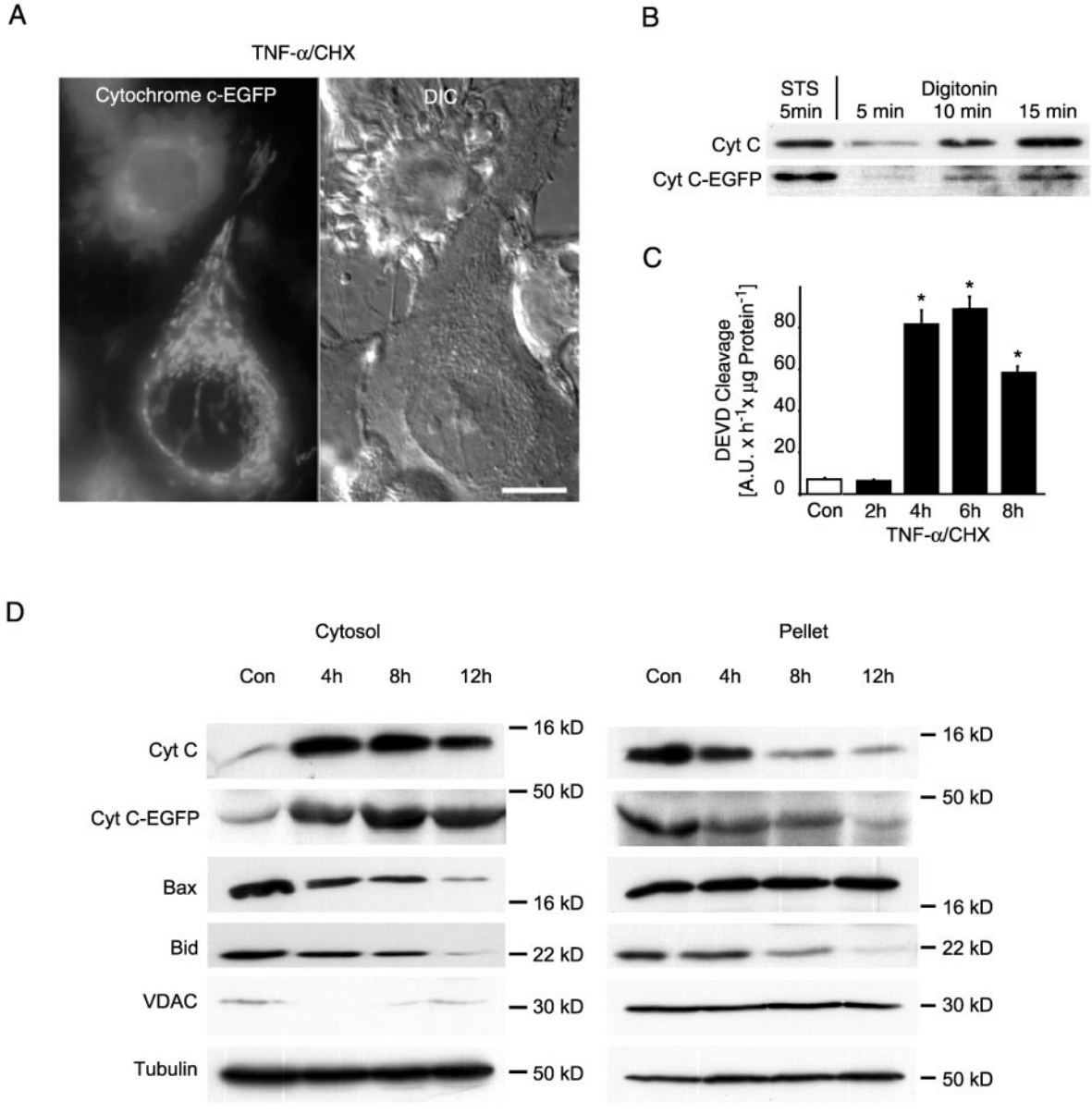

Fig. 1. TNF-α/CHX induces apoptosis and cytochrome *c* release in MCF-7/caspase-3 cells expressing cytochrome *c*-EGFP. A, epifluorescence images of MCF-7/Casp-3 cytochrome *c*-EGFP cells after treatment with 100 ng/ml TNF-α plus 1 μg/ml cycloheximide (TNF-α/CHX) for 6 h. The upper cell has released cytochrome *c*-EGFP. Differential interference contrast image (DIC, right image) showing the morphology of both cells. Upper cell shows a contracted cell body and membrane blebbing. Scale bar = 5 μm. B, EGFP-tagged cytochrome *c* is located within the outer mitochondrial membrane of MCF-7/Casp-3/cytochrome *c*-EGFP cells. The kinetics of cytochrome *c* and cytochrome *c*-EGFP release from mitochondria were analyzed after digitonin permeabilization (250 μg/ml, 4°C). At the indicated time points, soluble cytochrome *c* and cytochrome *c*-EGFP were detected in the supernatant by Western blotting. Cells treated with 3 μM STS for 4 h before digitonin permeabilization showed significant amounts of cytochrome *c* and cytochrome *c*-EGFP in the supernatant already after 5 min of permeabilization. Experiments were performed three times with similar results. C, caspase-3-like activity after treatment with 100 ng/ml TNF-α/CHX or vehicle. Caspase-3-like activity is shown as cleavage rate of DEVD substrate after 2 h, 4 h, 6 h, and 8 h of exposure to TNF-α/CHX. Cleavage of Ac-DEVD-AMC was monitored over 1 h. Data are means ± S.E.M. from $n = 8$ cultures per treatment. Experiments were performed three times with similar results. *, $P < 0.05$; difference from control cultures. A.U., arbitrary fluorescence units. D, subcellular distribution of cytochrome *c*, cytochrome *c*-EGFP, Bax, and full-length Bid at various time points after TNF-α/CHX stimulation detected by subcellular fractionation and immunoblotting. Blots were also incubated with an anti-VDAC antibody to detect contaminations of outer mitochondrial proteins in the cytosolic fractions. Anti-α-tubulin was used to ensure equal loading of samples. The experiment was repeated three times with similar results.

outer membrane proteins, or a mouse monoclonal anti-α-tubulin antibody (clone DM 1A; 1:1000, Sigma Chemie) to prove equal loading of the samples.

Measurement of Caspase Activity. After treatment with TNF-α/CHX, valinomycin, STS, or vehicle, cells were lysed in 200 μl of lysis buffer [10 mM Hepes, pH 7.4, 42 mM KCl, 5 mM $MgCl_2$, 1 mM phenylmethylsulfonyl fluoride, 0.1 mM EDTA, 0.1 mM EGTA, 1 mM DTT, 1 μg/ml pepstatin A, 1 μg/ml leupeptin, 5 μg/ml aprotinin, and 0.5% 3-(3-cholamidopropyldimethylammonio)-1-propane sulfonate (CHAPS)]. Fifty microliters of this lysate was added to 150 μl of reaction buffer (25 mM Hepes, 1 mM EDTA, 0.1% CHAPS, 10% sucrose, 3 mM DTT, pH 7.5, and 10 μM the caspase substrate Ac-DEVD-AMC). Accumulation of fluorescent AMC fluorescence was monitored over 120 min using an HTS fluorescent plate reader (PerkinElmer, Langen, Germany) (excitation, 380 nm; and emission, 465 nm). Fluorescence of blanks containing no cell lysate was subtracted from the values. Protein content was determined using the Pierce Coomassie Plus Protein Assay Reagent (KMF). Caspase activity is expressed as change in fluorescent units per microgram of protein and per hour.

Immunoprecipitation and Immunoblotting. MCF-7/Casp-3 cells were plated overnight at a density of 2×10^5 cells/cm^2 onto a 24-well tissue culture plate (Nunc GmbH & Co, Wiesbaden, Germany) and incubated for 6 h with vehicle [0.1% dimethyl sulfoxide (DMSO)], 3 μM STS, or 10 μM valinomycin in 300 μl of RPMI medium. As a control, untreated cells were lysed in 300 μl of PBS containing 2% Triton X-100 for 10 min. For the immunoprecipitation, the supernatants were centrifuged (10,000*g*, 10 min) to avoid contamination with cells or apoptotic bodies. In separate experiments, supernatants were also centrifuged at 100,000 g for 30 min, yielding similar results. Immunoprecipitation experiments were performed using a mouse monoclonal anti-cytochrome *c* antibody (6H2.B4, BD Pharmingen) in a final concentration of 0.5 μg/ml serum in a 4°C cold room, and rotation for 2 to 3 h. Subsequently, 30 μl of a 50% solution of protein G-Sepharose in PBS was added, and incubation was continued at 4°C in rotation for 1 h. Precipitates were harvested by short centrifugation (2000 rpm, 10 s) in a cold microcentrifuge and washed four times with cold washing buffer (20 mM Hepes, pH 7.4, 150 mM NaCl, 10% glycerol, and 0.1% Triton X-100 containing 1 μg/ml aprotinin and 1 μg/ml leupeptin). Proteins were eluted by boiling the precipitates in SDS-loading buffer supplemented with 5% 2-mercaptoethanol for 5 min, separated under reducing conditions on a 12% SDS-polyacrylamide gel, and subsequently transferred to a polyvinylidene difluoride membrane (Amersham Buchler, Braunschweig, Germany). Equal loading was confirmed by staining the proteins with Ponceau S. Membranes were blocked for 1 h with 5% nonfat dry milk powder in Tris-buffered saline containing 0.05% Tween 20 and then immunoblotted with a mouse monoclonal anti-cytochrome *c* antibody (7H8.2C12, BD Pharmingen) for 2 h. After the membranes were washed six times with TBST, they were incubated with anti-mouse peroxidase-conjugated secondary antibody for 1 h. Finally, the blots were washed and developed by enhanced chemiluminescent staining using ECL reagents (Amersham Buchler). Expression of cytochrome *c*-EGFP was verified by immunoblotting using a rabbit polyclonal antibody against GFP (CLONTECH). Therefore the immunoblot was stripped in standard stripping buffer (2% SDS, 62.5 mM Tris-HCl, and 100 mM 2-mercaptoethanol, pH 6.8) for 30 min at 60°C, washed twice in wash buffer for 10 min, and probed with the anti-GFP antibody diluted 1:1000 for 2 h.

Statistics. Data are given as means ± S.E.M. For statistical comparison, analysis of variance and subsequent Tukey's test were employed. *P* values less than 0.05 were considered to be statistically significant.

Results

EGFP-Tagged Cytochrome *c* Is Imported into Mitochondria and Released upon Digitonin Permeabilization. Epifluorescence microscopy of human breast carcinoma MCF-7/Casp-3 cells stably transfected with cytochrome *c*-EGFP revealed a typical filamentous mitochondrial cytochrome *c*-EGFP signal (Fig. 1A, bottom cell). Digitonin permeabilization of the outer mitochondrial membrane was performed to demonstrate the concomitant release of cytochrome *c* and cytochrome *c*-EGFP from the mitochondrial intermembrane space. A 5-min treatment with digitonin concentrations that have been reported to result in mitochondrial outer membrane permeabilization (250 and 500 μg/ml; Pedersen et al., 1978; Tanveer et al., 1996) triggered the release of endogenous cytochrome *c* (Fig. 1B and data not shown). Prolonged duration of the digitonin exposure led to an increase in the amount of cytochrome *c* released. Cytochrome *c*-EGFP was released upon digitonin permeabilization with very similar kinetics as endogenous cytochrome *c* (Fig. 1B). Both endogenous cytochrome *c* and cytochrome *c*-EGFP could also be increasingly detected in the supernatants of cells permeabilized for 5 min and pretreated for 4 h with 3 μM staurosporine. Treatment with digitonin concentrations that have been reported to permeabilize the mitochondrial matrix (2000–4000 μg/ml) caused a complete release within 5 min (data not shown). The release kinetics of cytochrome *c* and cytochrome *c*-EGFP indicated that EGFP-tagged cytochrome *c* is imported into mitochondria and located within the outer mitochondrial membrane.

Exposure to TNF-α/CHX Induces Mitochondrial Cytochrome *c* Release and Caspase Activity. Exposure of cytochrome *c*-EGFP-transfected MCF-7/Casp-3 cells to various concentrations of TNF-α supplemented with 1 μg/ml CHX induced caspase 3-like activity in a dose-dependent manner (Table 1), confirming cellular sensitivity of MCF-7 to TNF-α (Jänicke et al., 1998). To relate the time course of TNF-α/CHX-induced caspase activation with the kinetics of cytochrome *c* release, MCF-7/Casp-3 cells were treated with 100 ng/ml TNF-α/CHX for 2, 4, 6, and 8 h. The treatment caused a significant increase in caspase-3-like protease activity starting 4 h after onset (Fig. 1C). Parental caspase-3-deficient MCF-7 cells (Jänicke et al., 1998) did not show an increase in Ac-DEVD-AMC cleavage activity in response to TNF-α/CHX (data not shown). Treatment with TNF-α/CHX also induced morphological changes characteristic of apoptosis. (Fig. 1A, top cell). After 6–8 h of treatment, many cells

TABLE 1

TNF-α/CHX and STS induce caspase 3-like protease activity in MCF-7/Casp-3/Cytochrome c-EGFP cells

Cultures were treated for 6h with TNF-α/CHX, STS, or respective vehicle. CHX was given at a final concentration of 1 μg/ml. Cleavage of fluorigenic Ac-DEVD-AMC was monitored over 2 h using a fluorescent plate reader. Data are means ± S.E.M. from $n = 4$ cultures per treatment. Experiments were repeated two times with similar results.

Treatment	DEVD Cleavage Activity
	A.U./h/μg protein
Vehicle (PBS)	0.07 ± 0.04
10 ng/ml TNF-α + CHX	6.00 ± 0.34*
30 ng/ml TNF-α + CHX	10.17 ± 1.73*
100 ng/ml TNF-α + CHX	14.40 ± 1.06*
Vehicle (DMSO)	0.03 ± 0.03
0.3 μM STS	0.21 ± 0.20
1 μM STS	3.52 ± 0.68*
3 μM STS	11.86 ± 1.13*

A.U., arbitrary fluorescence units.
*, $p < 0.05$, difference from vehicle-treated control cells (analysis of variance and Tukeytest).

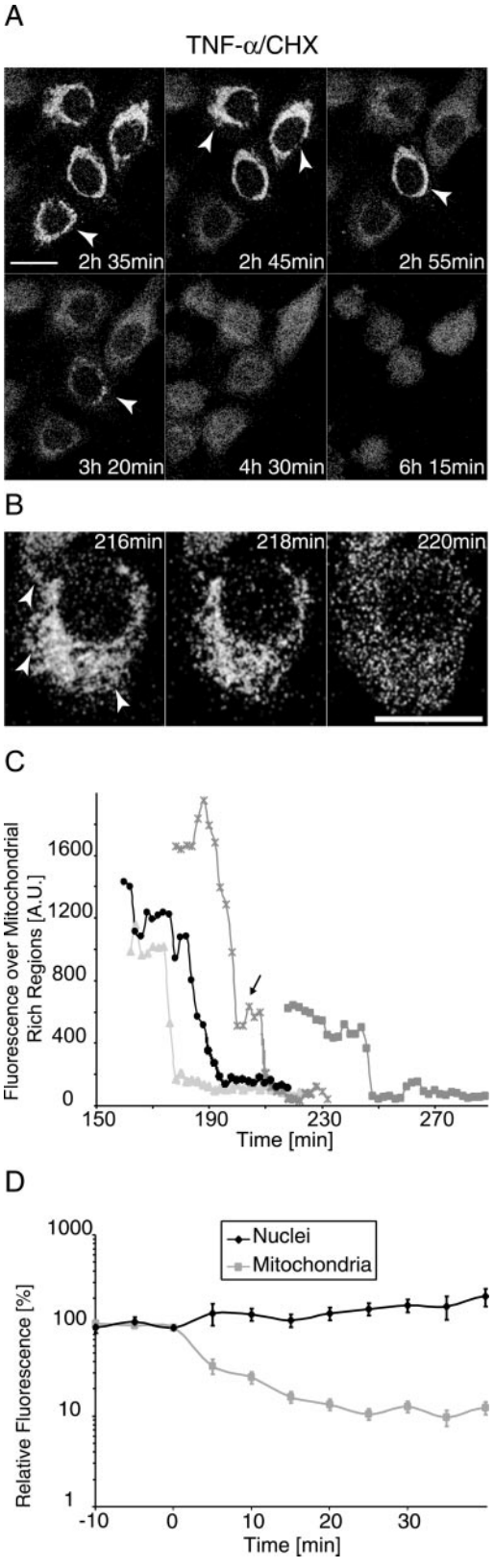

Fig. 2. Cytochrome *c*-EGFP is released very rapidly after exposure to TNF-α/CHX. Cells were exposed to TNF-α/CHX and monitored with a confocal laserscan. A, cytochrome *c*-EGFP release is not synchronized among cells. Six images of a 7-h time-lapse experiment (5-min sample rate) demonstrating the individual release of cytochrome *c*-EGFP in four cells and its consecutive distribution into the cytoplasm and nuclei. Arrows indicate cells that will have redistributed a EGFP-signal in the following image. Experiments have been repeated five times with similar results. Scale bar = 20 μm. B, coordinated release of cytochrome *c*-EGFP from mitochondria. Three zoomed confocal time-lapse images of a cell acquired at 2-min intervals. Arrows indicate mitochondria-rich regions with redistributed EGFP-signal in the following image. Scale bar = 20 μm. C, quantification of cytochrome *c*-EGFP fluorescence over mitochondria-rich regions. Note that the release event takes place within minutes, but can take distinct steps. Graph indicates the absolute fluorescence over mitochondria-rich regions of four individual cells. Images were taken at an interval of 5 min. Arrow indicates a 10-min intermediate halt of EGFP-signal redistribution. D, quantification of cytochrome *c*-EGFP release. Standardized graph showing relative fluorescence at different time points before and after the release event for mitochondria-rich regions and nuclei. Eleven time points per release event have been considered. Data are from $n = 25$ cells in five separate experiments acquired at 5-min sample rate. Note the semilogarithmic scale.

began to contract and showed extensive membrane blebbing. Epifluorescence microscopy revealed that the cytochrome *c*-EGFP signal was diffuse in these cells and distributed into the entire cytoplasm.

Subcellular fractionation experiments were used to confirm the concomitant release of endogenous cytochrome *c* and cytochrome *c*-EGFP from mitochondria in relation to caspase activation, Bax translocation, and Bid cleavage (Fig. 1D). As with the permeabilization experiments, the kinetics of redistribution to the cytosol were very similar for both proteins after treatment with 100 ng/ml TNF-α/CHX. High amounts of cytochrome *c* and cytochrome *c*-EGFP were already released after 4 h and correlated with the onset of TNF-α/CHX-induced caspase activation. The release was associated with translocation of Bax to the mitochondrial membrane and cleavage of Bid, as judged by a steady decrease in soluble Bax and full-length Bid in the cytosolic fractions. After 12 h both proteins were barely detectable in the cytosolic fractions.

TNF-α/CHX Induces Cytochrome *c*-EGFP Release in a Short Pulse. Our epifluorescence observations of cells treated with TNF-α/CHX seldomly revealed a transition from mitochondrial EGFP-signal to a diffuse cytoplasmic distribution state. To investigate the kinetics of cytochrome *c*-EGFP release, we monitored cytochrome *c*-EGFP-transfected MCF-7/Casp-3 cells with a time-lapse confocal laserscan microscope at a 5-min sample rate. Nuclei and parts of the cytoplasm of MCF-7/Casp-3 cells expressing cytochrome *c*-EGFP did not have a significant EGFP signal and therefore appeared dark. Incubation with TNF-α/CHX induced a rapid cytochrome *c*-EGFP release (Fig. 2A). Although no preceding change in cell morphology could be observed, MCF-7/Casp-3 cytochrome *c*-EGFP cells suddenly started to release cytochrome *c*-EGFP into the cytoplasm. The moment of release was individually programmed after a variable time period for each cell and was not synchronized among cells (Fig. 2A; see also Fig. 2C). In the majority of cells, TNF-α/CHX-induced cytochrome *c*-EGFP release was completed in less than 10 min. At first, the signal distributed equally within the cytoplasm solely leaving the nucleus unmarked. Approximately 30 min later, the signal appeared also in the nuclei and became equally distributed throughout the entire cell compartments (Fig. 2A). Control cultures treated with vehicle and monitored at a 5-min sample rate for up to 12 h did not show a redistribution of the EGFP signal (data not shown).

Digital confocal time-lapse images with 2-min intervals revealed no distinct starting point within a cell (Fig. 2B). Mitochondria, regardless of their position within the cell, began simultaneously to release their cytochrome *c*-EGFP. This rapid release enabled us to quantify fluorescence

changes over large mitochondria-rich regions identified before the release event. The fluorescence over the mitochondria-rich regions decreased drastically within minutes (Fig. 2C). Similar release kinetics were obtained using a method described by Goldstein and coworkers (2000), in which standard deviation of the cellular pixel intensity was employed as a measure of cytochrome *c*-GFP redistribution (data not shown). Interestingly, the overall fluorescence of individual cells decreased rapidly after the release of cytochrome *c*-EGFP.

To estimate mean kinetics for the cytochrome *c*-EGFP release in the TNF-α/CHX-treated cells, the mitochondrial fluorescence of individual cells before the release event was set to 100%, and the time point was set to 0 min. On average, the cytochrome *c*-EGFP fluorescence decreased in the mitochondria-rich regions within 10 to 20 min (Fig. 2D). On the other hand, the relative level of fluorescence in the nuclei increased slowly and doubled within 40 min, demonstrating the cytochrome *c*-EGFP signal redistribution (Fig. 2D).

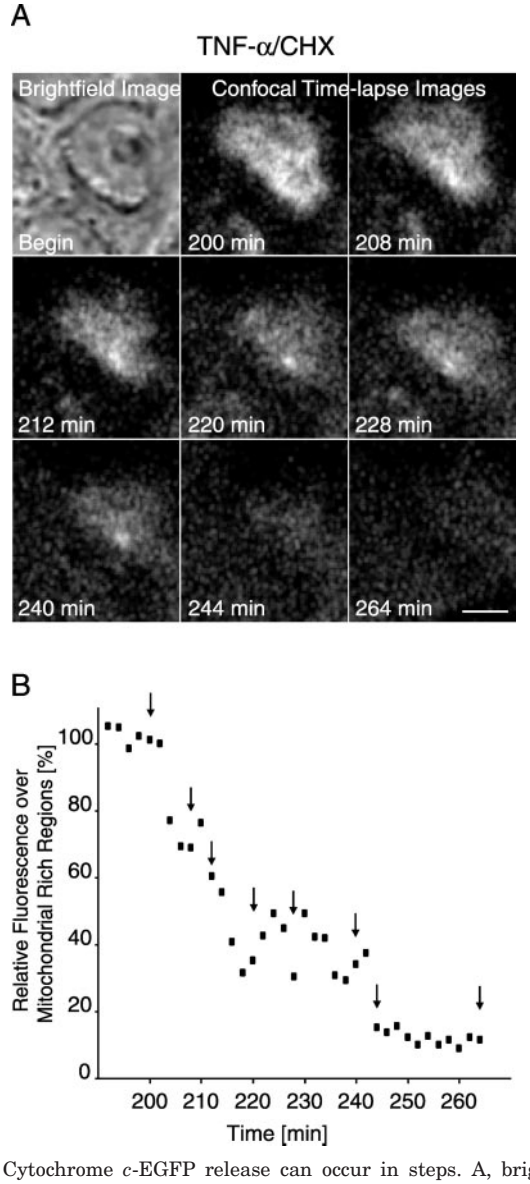

Fig. 3. Cytochrome *c*-EGFP release can occur in steps. A, brightfield image and eight consecutive confocal images of the same cell acquired at a 2-min sample rate after exposure to TNF-α/CHX. The fluorescence signal decreased in steps within an hour time frame. Brightfield images of the cell remained unchanged during the time course of data collection (not shown). Scale bar = 10 μm. B, quantification of the relative fluorescence over the mitochondria-rich regions of this cell, demonstrating the release kinetic in 2-min intervals. The EGFP-signal decreased in two distinct steps with a intermediate plateau 25 min in duration. Arrows indicate the amount of measured fluorescence in the shown images.

Cytochrome *c* Release in Steps. The confocal time-lapse images also showed that cells occasionally underwent a stepwise decrease in mitochondrial EGFP signal (see cell depicted by an arrow in Fig. 2C). A zoomed high magnification of a cell sampled at 2-min intervals is shown in Fig. 3A. After 200 min of TNF-α/CHX exposure, this cell started releasing cytochrome *c*-EGFP and reached a midpoint plateau (approximately 40% of the starting level) 12 min later. It remained at this level about 30 min before the signal finally decreased again to reach a bottom plateau of approximately 10% of the initial fluorescence (Fig. 3B). Although the first declining step took place within a short time frame, the intermediate step prolonged the release at least by 4-fold. Cytochrome *c*-EGFP release in steps could be detected in 13% of release events monitored (n = 10 experiments).

STS-Induced Cytochrome *c*-EGFP Release. We next investigated the response of cytochrome *c*-EGFP-transfected MCF-7/Casp-3 cells to the protein kinase inhibitor STS. Dose-response studies revealed that STS induced significant caspase 3-like activity at a concentration of 1 and 3 μM, but not at a concentration of 0.3 μM (Table 1). Confocal time-lapse experiments were performed in cells treated with 3 μM STS. Similar to the TNF-α/CHX treatment, the release of cytochrome *c*-EGFP began in each cell at an individual time point (Fig. 4A). In each release event, the absolute fluorescence signal of the mitochondria-rich regions decreased within minutes (Fig. 4B). Within an hour the EGFP-signal was equally distributed and could also be observed in the nucleus region. As observed with TNF-α/CHX, the cytochrome *c*-EGFP release frequently was exerted in two or more steps (Fig. 4B, arrows). On average, the EGFP signal decreased in the mitochondria-rich regions within 10 to 20 min in response to STS (Fig. 4E).

Cytochrome *c* Release Is Not Altered by Caspase Inhibition. Recently, a positive feedback loop of caspase-induced cytochrome *c* release has been suggested (Chen et al., 2000; Slee et al., 2000). Since both of these studies relied on bulk analysis, we were interested to determine the existence of caspase-dependent feedback amplification signals on the single cell level. STS-induced cytochrome *c* redistribution was monitored in the presence of 100 μM pan-specific caspase inhibitor zVAD-fmk. At this concentration, STS-induced caspase-3-like protease activity determined by Ac-DEVD-AMC cleavage was completely inhibited (data not shown). Cytochrome *c* was released with identical kinetics compared with control cells treated with STS alone (Fig. 4C and D). Quantification of time-lapse experiments with 5-min intervals (Fig. 4E) or 1-min intervals (Fig. 4F) revealed identical release kinetics. The 1-min interval scans also revealed no release starting point within cells (Fig. 2B).

Valinomycin Induces Cytochrome *c* Release and Caspase Activation. We then compared the effects of STS with those of valinomycin, a potassium ionophore that depolarizes mitochondria and that has been reported to induce the PTP (Inai et al., 1997; Furlong et al., 1998). Subcellular fractionation experiments revealed that both STS and valinomycin induced significant cytochrome *c* release into the

cytosolic compartment (Fig. 5, A and B). Release of cytochrome *c* after exposure to STS occurred within 4 h, confirming our previous confocal imaging data. In the case of valinomycin, cytochrome *c* could be detected in the cytosol after 12 h of treatment. Cytochrome *c* content increased further by 24 h of treatment. Subcellular fractionation experiments re-

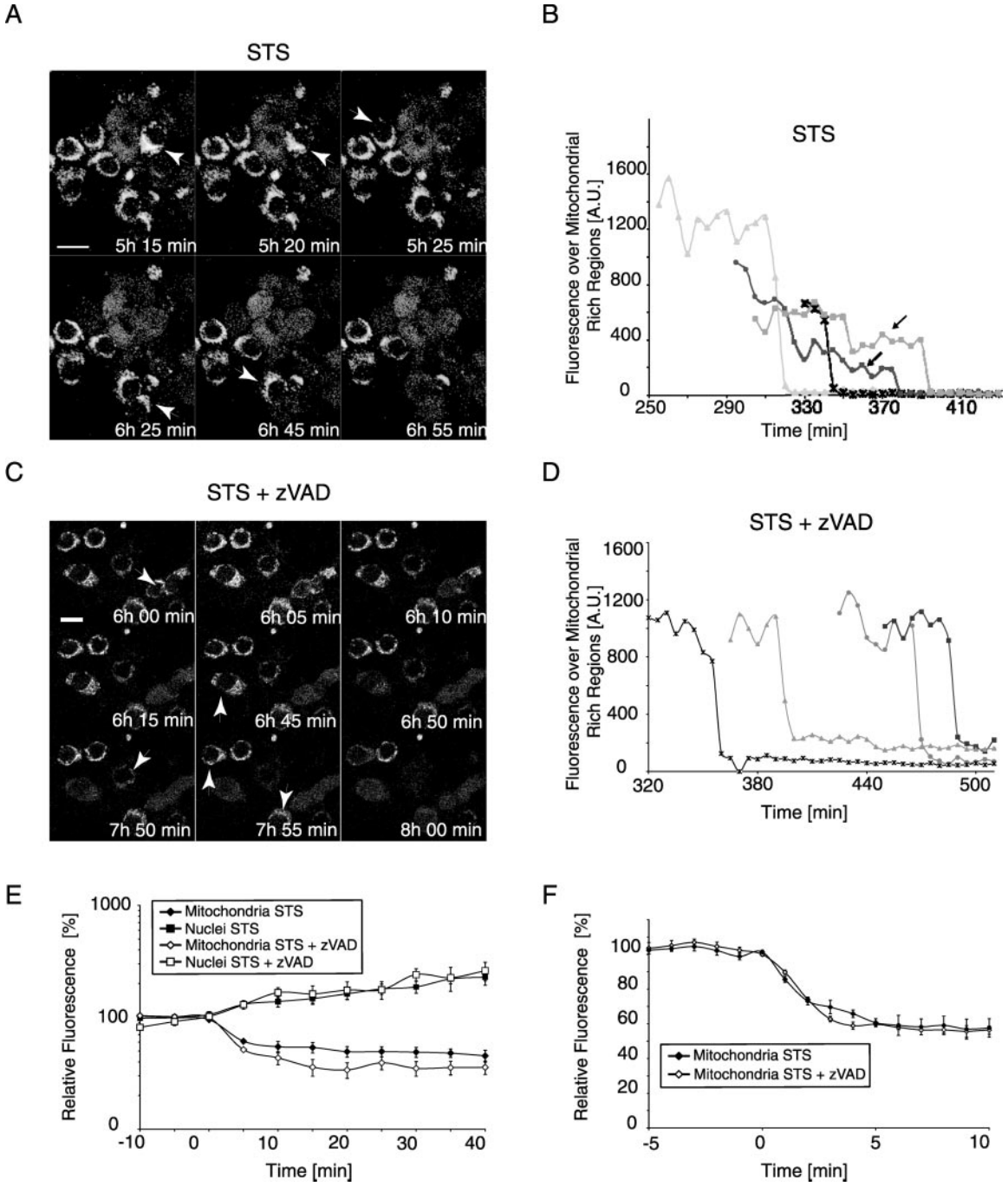

Fig. 4. Cytochrome *c*-EGFP release after exposure to STS. A, MCF-7/Casp-3 cytochrome *c*-EGFP cells release cytochrome *c*-EGFP within minutes after exposure to 3 μM STS. Release is not synchronized among the cells. Six confocal images of a 7-h time-lapse experiment (5-min sample rate) demonstrating the individual release events. Arrows indicate cells that will have redistributed EGFP-signal in the following image. Experiments have been repeated six times with similar results. Scale bar = 20 μm. B, cytochrome *c*-EGFP release takes place within minutes but proceeds frequently in steps. Graph indicates the absolute fluorescence of mitochondria-rich regions of four cells. Images were taken at an interval of 5 min. Arrows indicate a 30-min or 50-min intermediate halt of EGFP-signal redistribution, respectively. C, time course of cytochrome *c*-EGFP release after exposure to STS in the presence of 100 μM zVAD-fmk. Nine confocal images of a time-lapse experiment (at 5-min sample rate) are shown. Arrows indicate cells which will release cytochrome *c*-EGFP in the following image. Experiments have been repeated six times with similar results. D, cytochrome *c*-EGFP release takes place within minutes in cells treated simultaneously with 3 μM STS and 100 μM zVAD-fmk. E, quantification of cytochrome *c*-EGFP release kinetics after STS exposure in the presence or absence of 100 μM zVAD-fmk. Standardized graph showing relative fluorescence of mitochondria-rich regions and nuclei at two time points before and eight time points after the release event (5-min sample rate). Data are from n = 15 (with zVAD-fmk) and n = 14 (without zVAD-fmk) release events in three separate experiments each. Note the semilogarithmic scale. Better time resolution is given in F, where the release events were observed at 60-s intervals. Data are from n = 4 (with zVAD) and n = 5 (without zVAD) release events.

vealed that, in contrast to STS and TNF-α/CHX, cytochrome *c* release triggered by valinomycin was not associated with detectable translocation of Bax to the mitochondria. Bax translocation was also monitored in MCF-7 cells stably expressing DsRed-tagged Bax. Translocation of DsRed-bax occurred early in response to STS, but not in response to valinomycin (Fig. 5C). This was consistent with our findings on the redistribution of endogenous Bax (Fig. 5, A and B). Significant cytochrome *c* redistribution occurred simultaneously with the onset of caspase activation following both stimuli. STS caused an early increase in caspase activity after 4 h of treatment, after which time most of the cyto-

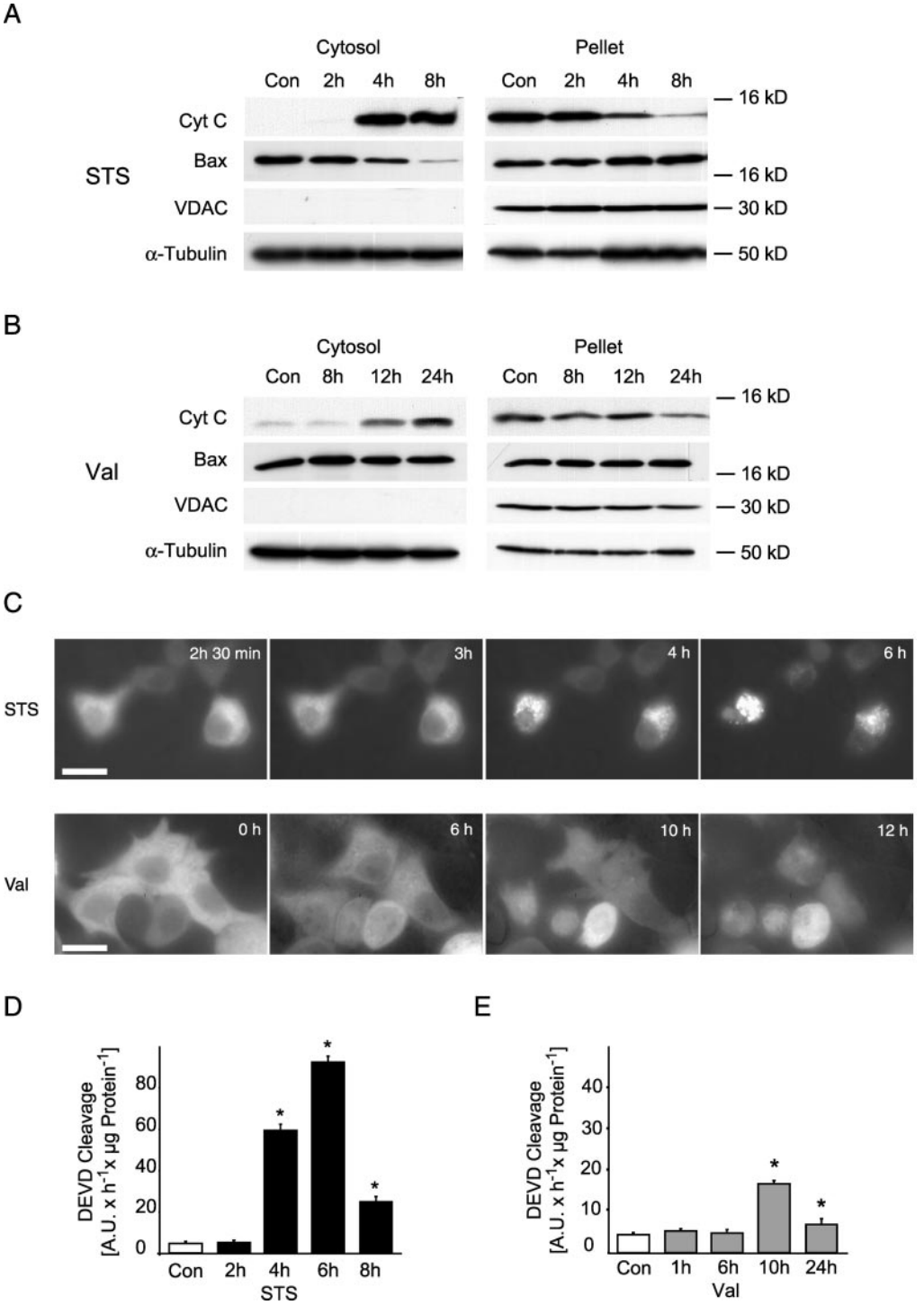

Fig. 5. Cytochrome *c* release, Bax translocation, and caspase activation in response to STS and valinomycin. A and B, cultured MCF-7/Casp-3 cytochrome *c*-EGFP were incubated with STS (3 μM) or valinomycin (10 μM), fractionated at various time points and analyzed by Western blotting with the indicated antibodies. Experiments were performed in triplicate with similar results. C, DsRed-bax redistribution in response to STS (3 μM) and valinomycin (10 μM). Scale bar = 20 μm. Experiments were performed in triplicate with similar results. D and E, caspase-3-like activity of MCF-7/Casp-3 cytochrome *c*-EGFP cells incubated with STS (3 μM) or valinomycin (10 μM) was measured by cleavage of the fluorogenic substrate Ac-DEVD-AMC. Activities are presented as increase in AMC fluorescence (in arbitrary fluorescence units) over 60 min/μg of protein. Data are means ± S.E.M. from $n = 8$ cultures. Experiments were repeated three times with similar results. Different from controls. *, $P < 0.05$.

chrome *c* had been released from the mitochondria (Fig. 5D). In response to valinomycin, caspase activation was more delayed, and the magnitude was less pronounced (Fig. 5E).

In addition to cytochrome *c*, the proapoptotic factor Smac has been reported to be released from the mitochondria during apoptosis (Du et al., 2000). Smac inhibits the family of inhibitor of apoptosis proteins (IAPs), which in turn inhibit caspase activation after the mitochondrial release of cytochrome. Smac was released into the cytosolic compartment after 4 and 8 h of STS treatment (Fig. 6A). In contrast, redistribution of Smac could not be observed after treatment with valinomycin, even after 24 h (Fig. 6B). Lack of Smac release could therefore account for the less efficient caspase activation after valinomycin treatment.

Valinomycin Induces Slow Cytochrome *c*-EGFP Release. We then monitored MCF-7/Casp-3 cells expressing cytochrome *c*-EGFP during the exposure to 10 μM valinomycin. In sharp contrast to the TNF-α/CHX and STS experiments, confocal time-lapse images revealed a slow redistribution of the cytochrome *c*-EGFP signal from mitochondria into the cytoplasm and nucleus. A zoomed high magnification of a cell sampled at 15-min intervals is shown in Fig. 7A. At the beginning, almost no fluorescence signal could be detected inside the nucleus region. Starting at 4 to 8 h and lasting up to 24 h, the distribution of the EGFP-signal alternated and lost its typical punctate mitochondrial pattern. Concomitantly, the fluorescence signal in the nucleus increased progressively. Significant matrix swelling was observed by confocal and epifluorescence microscopy before the release of cytochrome *c*-EGFP (data not shown).

Confocal time-lapse images of a field of MCF-7/casp-3 cells monitored at 15-min intervals over 24 h is shown in Fig. 7B. Note that all cells revealed a slow loss of the punctate cytochrome *c*-EGFP signal over several hours, and a slow redistribution into the nucleus. Control cells exposed to the vehicle and confocally monitored at 15-min intervals for up to 24 h did not exhibit any cytochrome *c*-EGFP signal redistribution (Fig. 7C).

Because cytochrome *c*-EGFP redistribution occurred over several hours and cells moved and changed morphologically, we could not evaluate the kinetics of the release event by quantifying mitochondrial EGFP fluorescence. However, increases in nuclear cytochrome *c*-EGFP fluorescence reflect increases in cytoplasmic cytochrome *c*-EGFP (Figs. 2D and 4E; Heiskanen et al., 1999); and therefore, nuclear fluorescence changes were quantified to estimate the release kinetics in response to valinomycin (Fig. 7D). Measurement of the fluorescence signal within the individual nuclear regions revealed an increase in the EGFP fluorescence starting 8 h after the onset of treatment and gradually increasing up to 16 h afterward (Fig. 7D). In contrast, nuclear fluorescence of vehicle-treated control cultures acquired at an identical sample rate did not increase during the 24-h time-lapse experiment.

Cytochrome *c* Secretion out of the Cell. All cells exposed to valinomycin for 24 h exhibited a diffuse cytochrome *c*-EGFP signal (Fig. 7B). Although some cells underwent typical apoptotic changes (rounding of the cell body, shrinkage), many cells with diffuse cytochrome *c*-EGFP remained morphologically unchanged for the entire experiment (Fig. 8A, brightfield images). Interestingly, most cells that demonstrated cytochrome *c*-EGFP redistribution also failed to take up the membrane-impermeant dye propidium iodide (Fig. 8A), indicating that the cells did not die by necrosis but were in fact viable.

Interestingly, cytochrome *c* release occurred not only out of the mitochondrial compartments, but also out of the cells into the medium (Fig. 8, B and C). MCF-7/Casp-3 cytochrome *c*-EGFP cells were treated for 6 h with valinomycin, STS, or vehicle. At this time point, both valinomycin and STS failed to take up the membrane-impermeant dye ethidium-homodimer (data not shown). Measurement of lactate dehydrogenase activity of the supernatants revealed that neither valinomycin nor STS caused a loss of plasma membrane integrity, indicating the absence of primary or secondary necrosis. We collected the supernatants and performed an immunoprecipitation with a monoclonal anti-cytochrome *c* antibody recognizing native cytochrome *c*. As a control, immunoprecipitation was performed using cell lysates from MCF-7/Casp-3 cytochrome *c*-EGFP cells. Subsequent Western blotting of precipitates and immunodetection with an antibody recognizing denatured cytochrome *c* detected both the endogenous (12.5 kDa) and the EGFP-conjugated cytochrome *c* (43 kDa) in the lysate control (Fig. 8B, Lysate). Interestingly, endogenous cytochrome *c* could be detected in the supernatants of valinomycin-treated, and to lesser extent of STS-treated, cultures (Fig. 8B). Vehicle-treated controls did not release significant amounts of cytochrome *c* into the supernatant. In subsequent experiments the differential kinetics of valinomycin- and STS-induced cytochrome *c* secretion were analyzed in more detail (Fig. 8C). Cytochrome *c* was detectable in the supernatant of valinomycin-treated cells already after 4 h (Fig. 8C) thus preceding caspase activation (Fig. 5E). Cytochrome *c* release into the extracellular compartment was more pronounced after 8 h and was associated with a corresponding decrease in the total cellular cytochrome *c* content. In contrast, significant cytochrome *c*

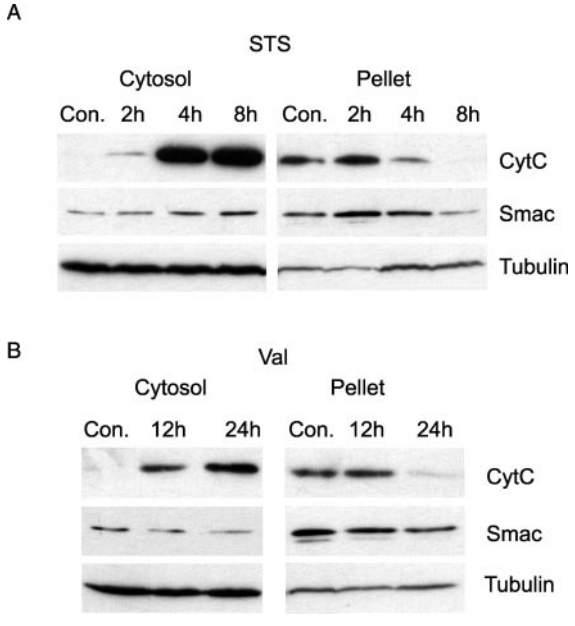

Fig. 6. Differential release of proapoptotic factors cytochrome *c* and Smac from the mitochondria. MCF-7/Casp-3 cytochrome *c*-EGFP cells were treated with 3 μM STS (A) or 10 μM valinomycin (B) and fractionated at the indicated time points. Redistribution of cytochrome *c* and Smac was analyzed by Western blotting. Con, vehicle-treated controls.

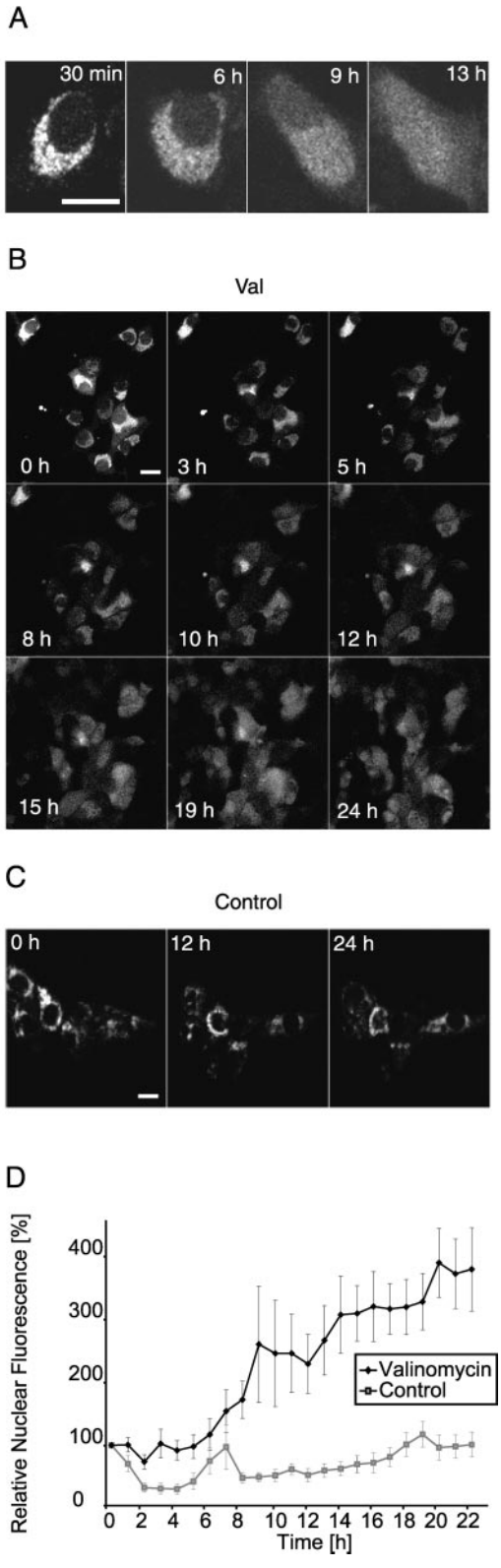

Fig. 7. Slow redistribution of cytochrome *c*-EGFP after exposure to valinomycin. A, confocal images of a single MCF-7/Casp-3 cytochrome *c*-EGFP cell in response to 10 μM valinomycin. Scale bar = 20 μm. B, valinomycin induces cytochrome *c*-EGFP release in a slow manner. Confocal time-lapse images reveal the slow redistribution of cytochrome *c*-EGFP within 1 day. Cells were exposed to 10 μM valinomycin for 24 h and scanned at a 15-min sample rate. Experiments have been performed in quadruple with similar results. C, in a control experiment, 0.1% DMSO-treated cells have been confocally monitored for 24 h at a 15-min sample rate. No EGFP-signal redistribution was observed. Scale bar = 20 μm. D, quantification of nuclear cytochrome *c*-EGFP fluorescence in response to valinomycin or vehicle. Nuclear fluorescence before the exposure was set to 100% for each cell. Data are means ± S.E.M. from n = 18 and n = 21 cells in three and two experiments, respectively.

secretion out of the cell did not occur until 8 h after treatment (Fig. 8C), i.e., after caspase 3-like activity had reached its peak (Fig. 5D).

Discussion

In the present study we have used time-lapse laserscan technologies to investigate the release kinetics of cytochrome *c*-EGFP in response to three apoptosis-inducing agents, i.e., TNF-α/CHX, staurosporine (STS), and valinomycin. In agreement with two earlier reports investigating cytochrome *c*-EGFP release during apoptosis (Heiskanen et al., 1999; Goldstein et al., 2000) our data demonstrate that cytochrome *c*-EGFP redistributes to the cytosol and nucleus during apoptosis and colocalizes with endogenous cytochrome *c* after its release. In contrast to these studies, however, our data indicate that cytochrome *c*-EGFP release in apoptosis is a kinetically variable event: TNF-α/CHX- and STS-induced cytochrome *c*-EGFP release occurred rapidly, within minutes, whereas the valinomycin-induced cytochrome *c*-EGFP release occurred slowly, over several hours.

The release kinetics after treatment with TNF-α/CHX or staurosporine were similar, although two different apoptotic pathways were induced (Figs. 2 and 4). The release events consisted of a short pulse leading to almost total depletion of mitochondrial cytochrome *c*-EGFP or at least to a much lower level. Our time-lapse images at 5-, 2-, or 1-min intervals did not reveal a local starting point within a cell (Fig. 2B), indicating that the release was triggered for each mitochondrion in a stochastic manner. It remains possible, however, that we missed release starting points if the release event was particularly quick. The coordinated release of cytochrome *c* after exposure to TNF-α/CHX or STS may be caused by activation of proapoptotic Bcl-2 family members Bax and Bak and their subsequent oligomerization in the outer mitochondrial membrane leading to channel formation and an outer membrane permeability increase in the gross majority of mitochondria (Eskes et al., 1998; Goping et al., 1998; Wei et al., 2001). In death receptor-mediated apoptosis, homo-oligomerization of Bax or Bak is triggered by increasing cytosolic concentrations of the caspase-activated BH3-only Bcl-2 family member tBid (Li et al., 1998; Luo et al., 1998; Desagher et al., 1999; Perez and White, 2000; Wei et al., 2001). Decrease in cytosolic and mitochondrial full-length Bid could be detected in response to TNF-α/CHX (Fig. 1D). TNF-α/CHX also caused a significant decrease in Bax content in the cytosolic fraction, but the increase in the mitochondrial fraction was not as pronounced. It is possible that proapoptotic Bak plays the prominent role in TNF-α/CHX -induced cytochrome *c* release in MCF-7 cells. In contrast, little is known about the upstream signaling events activating Bax and Bak in STS-induced apoptosis. Bax translocation to mitochondria could be clearly detected after treatment with STS (Figs. 1D and 5A).

Interestingly, the release event could be taken in multiple steps (Figs. 2C, 3B, and 4B). Although cytochrome *c*-EGFP release in steps may not necessarily alter the overall kinetics of caspase activation, it might reflect the existence of positive

feedback loops that may be required for the amplification of the apoptotic signal as determined in bulk studies (Chen et al., 2000; Slee et al., 2000). However, the kinetics of STS-induced cytochrome *c* release were not affected by zVAD-fmk, suggesting caspase-independent feedback mechanisms of cytochrome *c* release (Fig. 4, E and F). Interestingly, microinjection of apoptosis-inducing factor (AIF) has been shown to trigger cytochrome *c* release in a caspase-independent manner (Loeffler et al., 2001) and could thus represent an alternative positive feedback loop. Otherwise, cytochrome *c*-EGFP release in steps may be due to a reorganization of cristae during apoptotic execution (Frey and Mannella, 2000). Cytochrome *c* in the intracristal space may initially not be completely accessible to outer membrane permeabilization and may thus require a reorganization of cristae for a complete release.

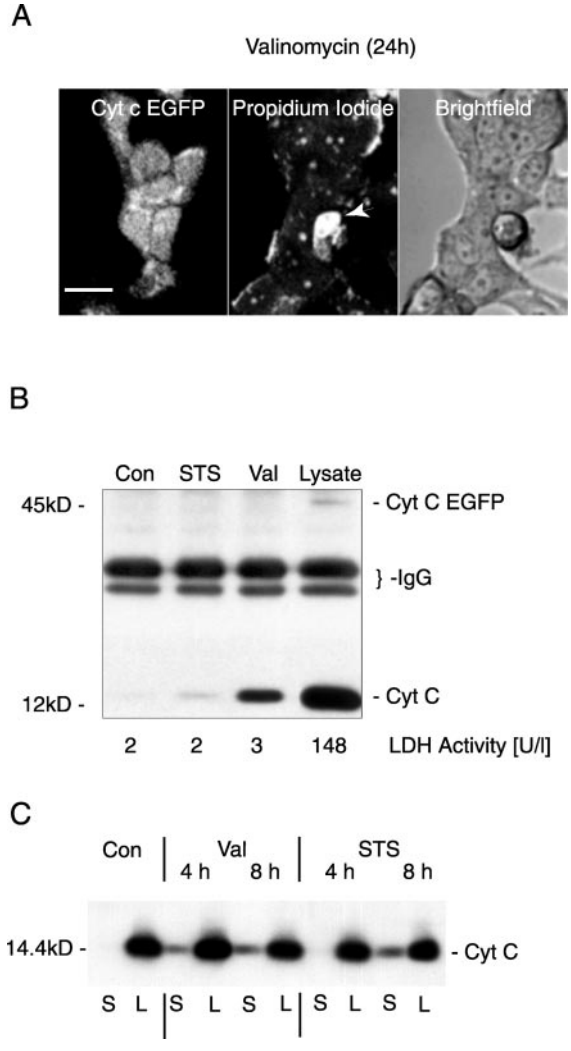

Fig. 8. A, MCF-7/Casp-3 cytochrome *c*-EGFP cells exposed to 10 μM valinomycin for 24 h and stained with propidium iodide. Note that all cells except one excluded propidium iodide despite complete cytochrome *c*-EGFP redistribution. B, release of cytochrome *c* into the extracellular compartment. MCF-7/Casp-3 cytochrome *c*-EGFP cells were exposed to vehicle (0.1% DMSO), 3 μM STS, or 10 μM valinomycin (Val) for 6 h. As a positive control for immunoprecipitation, untreated cultures were lysed with 0.5% Triton X-100. Supernatants and cell lysate were immunoprecipitated with an antibody against native cytochrome *c*. A duplicate experiment yielded comparable results. C, time course of cytochrome *c* secretion and relative amount of cellular to secreted cytochrome *c*. MCF-7/Casp-3 cytochrome *c*-EGFP cells were treated with 3 μM STS or 10 μM valinomycin (Val) for 4 or 8 h. Supernatants or whole cell lysates of the individual cultures were immunoprecipitated and cytochrome *c* detected by Western blotting. S, supernatant; L, whole cell lysate; Con, vehicle-treated control.

After the release of cytochrome *c*-EGFP, total cellular fluorescence decreased. It is unlikely that these changes are due to caspase-mediated degradation of cytochrome *c*-EGFP, as a similar decrease in fluorescence was noted in STS-exposed cultures treated with the broad spectrum caspase inhibitor, zVAD-fmk (Fig. 4C). Cytosolic acidification may contribute to the decrease in EGFP signal, but would be expected to occur less rapidly. Moreover, the drop in cytosolic pH observed during apoptosis does not fall below 7.0 (Matsuyama et al., 2000), a change in pH that only minimally affects EGFP fluorescence (Kneen et al., 1998). Instead, a more likely explanation for the observed decrease in overall fluorescence is the enhanced dynamic quenching due to the increased accessibility of released cytochrome *c*-EGFP to molecules interfering with excited EGFP and corresponding decrease in quantum yield of EGFP fluorescence after the release of cytochrome *c*-EGFP into the cytosolic compartment. Likewise, DsRed-Bax fluorescence increased after its translocation to mitochondria (Fig. 5C).

In contrast to TNF-α/CHX and STS, valinomycin induced slow cytochrome *c* redistribution over several hours that was independent of Bax translocation (Fig. 5). Valinomycin has been shown to trigger PTP opening (Inai et al., 1997; Furlong et al., 1998), an event that is known to be individually set for each mitochondrion (Nieminen et al., 1995; Lemasters et al., 1999). As a result, only a slow accumulation of cytoplasmic cytochrome *c* may occur over time. Valinomycin-induced cytochrome *c* release induced little caspase-3-like protease activity in MCF-7/Casp-3 cells (Fig. 5E). Valinomycin depolarizes mitochondria (Inai et al., 1997; Furlong et al., 1998), and could thus arrest caspase activation by inhibiting mitochondrial ATP production (Eguchi et al., 1997; Leist et al., 1997). However, cells were able to survive valinomycin-induced cytochrome *c* release for up to 2 days (Fig. 8A and authors' unpublished data). It is also conceivable that a rapid and complete release of cytochrome *c* might be a prerequisite to efficiently activate apoptosis. Interestingly, a rapid pulse is also achieved by microinjecting cytochrome *c* into the cytoplasm, a procedure that has been shown to result in activation of the caspase cascade (Chauhan et al., 1997; Li et al., 1997a). Moreover, the amount of microinjected cytochrome *c* required to induce cell death is similar to the estimated total cellular cytochrome *c* content (Chauhan et al., 1997; Li et al., 1997a). Cytochrome *c* could also be detected in the culture medium after treatment with valinomycin before the loss of plasma membrane integrity (Fig. 8B). It is conceivable that release of cytochrome *c* into the extracellular compartment may limit apoptosis activation. Interestingly, valinomycin and other apoptosis-inducing stimuli decrease intracellular K^+ levels (Bortner et al., 1997), a precondition that has been shown to trigger secretion of small proteins that lack an endoplasmic reticulum/secretion signal sequence (Rubartelli et al., 1990).

In addition to cytochrome *c*, Smac was released into the cytosol upon STS treatment (Fig. 6A). However, concomitant Smac release from the mitochondria was not traceable after valinomycin exposure (Fig. 6B). The absence of cytoplasmic Smac, which activates apoptosis by counteracting the inhibitory function of IAPs, might account for the less potent

apoptosis induction by valinomycin. To our knowledge, this is the first example of differential Smac and cytochrome *c* release from mitochondria.

In conclusion, our study demonstrates that cytochrome *c* release in drug-induced apoptosis is a kinetically variable event. Mitochondria are able to release cytochrome *c* rapidly and completely, in one or more steps, or slowly over several hours. The kinetics of cytochrome *c* release from mitochondria, co-release of Smac, as well as the subsequent spatial equilibration of cytochrome *c* after its release may influence the cell's decision to initiate an apoptotic cell death program. Drugs that accelerate or inhibit cytochrome *c* release may represent useful tools for the treatment of cancer, as well as ischemic and degenerative disorders.

Acknowledgments

We thank Christiane Schettler for technical assistance and Dr. Reiner Jänicke for the generous gift of the MCF-7/Casp-3 cell line.

References

Bortner CD, Hughes FM Jr, and Cidlowski JA (1997) A primary role for K+ and Na+ efflux in the activation of apoptosis. *J Biol Chem* **272:**32436–32442.

Bossy-Wetzel E, Newmeyer DD, and Green DR (1998) Mitochondrial cytochrome *c* release in apoptosis occurs upstream of DEVD-specific caspase activation and independently of mitochondrial transmembrane depolarization. *EMBO J* **17:**37–49.

Chauhan D, Pandey P, Ogata A, Teoh G, Krett N, Halgren R, Rosen S, Kufe D, Kharbanda S, and Anderson K (1997) Cytochrome *c*-dependent and -independent induction of apoptosis in multiple myeloma cells. *J Biol Chem* **272:**29995–29997.

Chen Q, Gong B, and Almasan A (2000) Distinct stages of cytochrome *c* release from mitochondria: evidence for a feedback amplification loop linking caspase activation to mitochondrial dysfunction in genotoxic stress induced apoptosis. *Cell Death Diff* **7:**227–233.

Desagher S, Osen-Sand A, Nichols A, Eskes R, Montessuit S, Lauper S, Maundrell K, Antonsson B, and Martinou JC (1999) Bid-induced conformational change of Bax is responsible for mitochondrial cytochrome *c* release during apoptosis. *J Cell Biol* **144:**891–901.

Du C, Fang M, Li Y, Li L, and Wang X (2000) Smac, a mitochondrial protein that promotes cytochrome *c*-dependent caspase activation by eliminating IAP inhibition. *Cell* **102:**33–42.

Eguchi Y, Shimizu S, and Tsujimoto Y (1997) Intracellular ATP levels determine cell death fate by apoptosis or necrosis. *Cancer Res* **57:**1835–1840.

Eskes R, Antonsson B, Osen-Sand A, Montessuit S, Richter C, Sadoul R, Mazzei G, Nichols A, and Martinou JC (1998) Bax-induced cytochrome *c* release from mitochondria is independent of the permeability transition pore but highly dependent on Mg2+ ions. *J Cell Biol* **143:**217–224.

Frey TG and Mannella CA (2000) The internal structure of mitochondria. *Trends Biochem Sci* **25:**319–324.

Furlong IJ, Lopez Mediavilla C, Ascaso R, Lopez Rivas A, and Collins MK (1998) Induction of apoptosis by valinomycin: mitochondrial permeability transition causes intracellular acidification. *Cell Death Diff* **5:**214–221.

Goldstein JC, Waterhouse NJ, Juin P, Evan GI, and Green DR (2000) The coordinate release of cytochrome *c* during apoptosis is rapid, complete and kinetically invariant. *Nat Cell Biol* **2:**156–162.

Goping IS, Gross A, Lavoie JN, Nguyen M, Jemmerson R, Roth K, Korsmeyer SJ, and Shore GC (1998) Regulated targeting of BAX to mitochondria. *J Cell Biol* **143:**207–215.

Heiskanen KM, Bhat MB, Wang HW, Ma J, and Nieminen AL (1999) Mitochondrial depolarization accompanies cytochrome *c* release during apoptosis in PC6 cells. *J Biol Chem* **274:**5654–5658.

Inai Y, Yabuki M, Kanno T, Akiyama J, Yasuda T, and Utsumi K (1997) Valinomycin induces apoptosis of ascites hepatoma cells (AH-130) in relation to mitochondrial membrane potential. *Cell Struct Funct* **22:**555–563.

Jänicke RU, Sprengart ML, Wati MR, and Porter AG (1998) Caspase-3 is required for DNA fragmentation and morphological changes associated with apoptosis. *J Biol Chem* **273:**9357–9360.

Kluck RM, Esposti MD, Perkins G, Renken C, Kuwana T, Bossy-Wetzel E, Goldberg M, Allen T, Barber MJ, Green DR, et al. (1999) The pro-apoptotic proteins, Bid and Bax, cause a limited permeabilization of the mitochondrial outer membrane that is enhanced by cytosol. *J Cell Biol* **147:**809–822.

Kneen M, Farinas J, Li Y, and Verkman AS (1998) Green fluorescent protein as a noninvasive intracellular pH indicator. *Biophys J* **74:**1591–1599.

Krammer PH (1999) CD95(APO-1/Fas)-mediated apoptosis: live and let die. *Adv Immunol* **71:**163–210.

Leist M, Single B, Castoldi AF, Kuhnle S, and Nicotera P (1997) Intracellular adenosine triphosphate (ATP) concentration: a switch in the decision between apoptosis and necrosis. *J Exp Med* **185:**1481–1486.

Lemasters JJ, Qian T, Bradham CA, Brenner DA, Cascio WE, Trost LC, Nishimura Y, Nieminen AL, and Herman B (1999) Mitochondrial dysfunction in the pathogenesis of necrotic and apoptotic cell death. *J Bioenerg Biomembr* **31:**305–319.

Li F, Srinivasan A, Wang Y, Armstrong RC, Tomaselli KJ, and Fritz LC (1997a) Cell-specific induction of apoptosis by microinjection of cytochrome *c*: Bcl-xL has activity independent of cytochrome *c* release. *J Biol Chem* **272:**30299–30305.

Li H, Zhu H, Xu CJ, and Yuan J (1998) Cleavage of BID by caspase 8 mediates the mitochondrial damage in the Fas pathway of apoptosis. *Cell* **94:**491–501.

Li K, Li Y, Shelton JM, Richardson JA, Spencer E, Chen ZJ, Wang X, and Williams RS (2000) Cytochrome *c* deficiency causes embryonic lethality and attenuates stress-induced apoptosis. *Cell* **101:**389–399.

Li P, Nijhawan D, Budihardjo I, Srinivasula SM, Ahmad M, Alnemri ES, and Wang X (1997b) Cytochrome *c* and dATP-dependent formation of Apaf-1/caspase-9 complex initiates an apoptotic protease cascade. *Cell* **91:**479–489.

Liu X, Kim CN, Yang J, Jemmerson R, and Wang X (1996) Induction of apoptotic program in cell-free extracts: requirement for dATP and cytochrome *c*. *Cell* **86:**147–157.

Loeffler M, Daugas E, Susin SA, Zamzami N, Metivier D, Nieminen AL, Brothers G, Penninger JM, and Kroemer G (2001) Dominant cell death induction by extramitochondrially targeted apoptosis-inducing factor. *FASEB J* **15:**758–767.

Luo X, Budihardjo I, Zou H, Slaughter C, and Wang X (1998) Bid, a Bcl2 interacting protein, mediates cytochrome *c* release from mitochondria in response to activation of cell surface death receptors. *Cell* **94:**481–490.

Marzo I, Brenner C, Zamzami N, Jurgensmeier JM, Susin SA, Vieira HL, Prevost MC, Xie Z, Matsuyama S, Reed JC, and Kroemer G (1998) Bax and adenine nucleotide translocator cooperate in the mitochondrial control of apoptosis. *Science (Wash DC)* **281:**2027–2031.

Matsuyama S, Llopis J, Deveraux QL, Tsien RY, and Reed JC (2000) Changes in intramitochondrial and cytosolic pH: early events that modulate caspase activation during apoptosis. *Nat Cell Biol* **2:**318–325.

Nieminen AL, Saylor AK, Tesfai SA, Herman B, and Lemasters JJ (1995) Contribution of the mitochondrial permeability transition to lethal injury after exposure of hepatocytes to t-butylhydroperoxide. *Biochem J* **307:**99–106.

Pedersen PL, Greenawalt JW, Reynafarje B, Hullihen J, Decker GL, Soper JW, and Bustamante E (1978) Preparation and characterization of mitochondria and submitochondrial particles of rat liver and liver-derived tissues. *Methods Cell Biol* **20:**411–481.

Perez D and White E (2000) TNF-alpha signals apoptosis through a bid-dependent conformational change in Bax that is inhibited by E1B 19K. *Mol Cell* **6:**53–63.

Rubartelli A, Cozzolino F, Talio M, and Sitia R (1990) A novel secretory pathway for interleukin-1 beta, a protein lacking a signal sequence. *EMBO J* **9:**1503–1510.

Saito M, Korsmeyer SJ, and Schlesinger PH (2000) BAX-dependent transport of cytochrome *c* reconstituted in pure liposomes. *Nat Cell Biol* **2:**553–555.

Shimizu S, Narita M, and Tsujimoto Y (1999) Bcl-2 family proteins regulate the release of apoptogenic cytochrome *c* by the mitochondrial channel VDAC. *Nature (Lond)* **399:**483–487.

Slee EA, Keogh SA, and Martin SJ (2000) Cleavage of BID during cytotoxic drug and UV radiation-induced apoptosis occurs downstream of the point of Bcl-2 action and is catalysed by caspase-3: a potential feedback loop for amplification of apoptosis-associated mitochondrial cytochrome *c* release. *Cell Death Diff* **7:**556–565.

Tanveer A, Virji S, Andreeva L, Totty NF, Hsuan JJ, Ward JM, and Crompton M (1996) Involvement of cyclophilin D in the activation of a mitochondrial pore by Ca^{2+} and oxidant stress. *Eur J Biochem* **238:**166–172.

Wei MC, Lindsten T, Mootha VK, Weiler S, Gross A, Ashiya M, Thompson CB, and Korsmeyer SJ (2000) tBID, a membrane-targeted death ligand, oligomerizes BAK to release cytochrome *c*. *Genes Dev* **14:**2060–2071.

Wei MC, Zong WX, Cheng EH, Lindsten T, Panoutsakopoulou V, Ross AJ, Roth KA, MacGregor GR, Thompson CB, and Korsmeyer SJ (2001) Proapoptotic BAX and BAK a requisite gateway to mitochondrial dysfunction and death. *Science (Wash DC)* **292:**727–730.

Zou H, Henzel WJ, Liu X, Lutschg A, and Wang X (1997) Apaf-1, a human protein homologous to *C. elegans* CED-4, participates in cytochrome *c*-dependent activation of caspase-3. *Cell* **90:**405–413.

Address correspondence to: Dr. Donat Kögel, Interdisciplinary Center for Clinical Research (IZKF), Research Group "Apoptosis and Cell Death," Faculty of Medicine, Westphalian Wilhelms-University, Röntgenstrasse 21, D-48149 Münster, Germany. E-mail: koegel@uni-muenster.de